Nuclear Instruments and Methods in Physics Research B 291 (2012) 29–37

Contents lists available at SciVerse ScienceDirect

Nuclear Instruments and Methods in Physics Research B

journal homepage: www.elsevier.com/locate/nimb

Performance of a high repetition pulse rate laser system for in-gas-jet laser ionization studies with the Leuven laser ion source @ LISOL

R. Ferrer [a,*], V.T. Sonnenschein [d], B. Bastin [c], S. Franchoo [f], M. Huyse [a], Yu. Kudryavtsev [a], T. Kron [b], N. Lecesne [c], I.D. Moore [d], B. Osmond [c], D. Pauwels [g], D. Radulov [a], S. Raeder [b,1], L. Rens [a], M. Reponen [d], J. Roßnagel [b], H. Savajols [c], T. Sonoda [e], J.C. Thomas [c], P. Van den Bergh [a], P. Van Duppen [a], K. Wendt [b], S. Zemlyanoy [h]

[a] Instituut voor Kern- en Stralingsfysica, KU Leuven, Celestijnenlaan 200D, B-3001 Leuven, Belgium
[b] Institut für Physik, Universität Mainz, D-55128 Mainz, Germany
[c] GANIL, CEA/DSM-CNRS/IN2P3, B.P. 55027, 14076 Caen, France
[d] Department of Physics, University of Jyväskylä, P.O. Box 35 (YFL), FI-40014 Jyväskylä, Finland
[e] RIKEN, 2-1 Hirosawa, Wako, Saitama 351-0198, Japan
[f] Institut de Physique Nucléaire (IPN) d'Orsay, 91406 Orsay, Cedex, France
[g] SCK·CEN, Belgian Nuclear Research Center, Boeretang 200, 2400 Mol, Belgium
[h] Joint Institute for Nuclear Research, 141980 Dubna, Russia

ARTICLE INFO

Article history:
Received 10 July 2012
Received in revised form 18 August 2012
Available online 18 September 2012

Keywords:
Resonance ionization
Laser ion source
Laser repetition rate
Gas cell
Gas jet

ABSTRACT

The laser ionization efficiency of the Leuven gas cell-based laser ion source was investigated under on- and off-line conditions using two distinctly different laser setups: a low-repetition rate dye laser system and a high-repetition rate Ti:sapphire laser system. A systematic study of the ion signal dependence on repetition rate and laser pulse energy was performed in off-line tests using stable cobalt and copper isotopes. These studies also included in-gas-jet laser spectroscopy measurements on the hyperfine structure of ^{63}Cu. A final run under on-line conditions in which the radioactive isotope ^{59}Cu ($T_{1/2}$ = 81.5 s) was produced, showed a comparable yield of the two laser systems for in-gas-cell ionization. However, a significantly improved time overlap by using the high-repetition rate laser system for in-gas-jet ionization was demonstrated by an increase of the overall duty cycle, and at the same time, pointed to the need for a better shaped atomic jet to reach higher ionization efficiencies.

1. Introduction

The Leuven Isotope Separator On-Line (LISOL) facility at the Cyclotron Research Center (CRC) Louvain-la-Neuve [1] produces purified rare ion beams using resonant laser ionization of reaction products thermalized in a buffer-gas cell [2,3]. After almost two decades of operation, high-purity radioactive ion beams of more than 15 different elements have been obtained exploiting various production mechanisms including light- and heavy-fusion evaporation reactions [4,5], proton-induced fission [6], and the spontaneous fission of ^{252}Cf [7]. Thermalized ion beams of rare species are extracted from the Leuven gas cell in a supersonic jet, transported by a radiofrequency (RF) ion guide towards the mass separator, and finally sent to the detector station.

In addition to the routinely performed nuclear-decay-spectroscopy studies, the recent upgrade of the LISOL setup with a novel gas cell concept [8] has allowed in-source laser spectroscopy studies of neutron-deficient $^{57-59}$Cu [9,10] and $^{97-102}$Ag [11] isotopes. These measurements have become feasible owing to the enhanced selectivity of the apparatus, which has allowed in-gas-cell laser spectroscopy on exotic species with count rates as low as 6 ions/s for ^{57}Cu ($T_{1/2}$ = 200 ms) or 1 ion/s for ^{97}Ag, both representing interesting semi-magic nuclei (N = 28 and 50, respectively).

In laser-spectroscopy experiments spectral linewidths are required to be as close as possible to the intrinsic natural linewidths of the atomic transitions investigated. For in-gas-cell laser spectroscopy, however, the obtained linewidths result from the convolution of four components: the Doppler broadening caused by the atom velocity distribution, the pressure broadening (and additionally pressure shift) induced by collisions with the surrounding gas, the laser-power broadening, and the intrinsic bandwidth of the laser.

* Corresponding author. Tel.: +32 16327271; fax: +32 16327985.
E-mail address: Rafael.Ferrer@fys.kuleuven.be (R. Ferrer).
[1] Present address: TRIUMF, 4004 Wesbrook Mall Vancouver, BC, Canada V6T 2A3.

0168-583X/$ - see front matter © 2012 Elsevier B.V. All rights reserved.
http://dx.doi.org/10.1016/j.nimb.2012.08.023

Following the earlier results obtained at LISOL by gas-cell laser spectroscopy it becomes clear that the spectral resolution is mainly limited by the inherent pressure broadening. Hence, for the successful study of atomic properties of elements with particularly small hyperfine splitting and/or high sensitivity to atomic collisions, as observed in practice, e.g., on the tin isotopes around $A = 100$, a novel approach such as in-gas-jet laser spectroscopy would be the technique of choice. In this method, laser ionization takes place in the supersonic jet expanding out of the gas cell. The adiabatic expansion into a lower pressure regime results in an important reduction of the Doppler and pressure broadening up to the point where the laser bandwidth becomes the primary limitation for the final attainable resolution. The feasibility of in-gas-jet laser spectroscopy was demonstrated in previous experiments at LISOL [12]. In those measurements the advantages of this technique in view of the realization of spectroscopic studies and of the enhancement of the ion beam purity (LIST mode [13]) were evaluated and compared to the results obtained under equal conditions by in-gas-cell laser spectroscopy. The first results obtained in Ref. [12] proved that in-gas-jet laser spectroscopy can meet the requirements of superior selectivity and resolution.

To obtain optimum experimental conditions for the application of in-gas-jet spectroscopy the overlap efficiency between the laser light and the atoms in the gas jet must be maximized by the temporal and the geometrical overlap parameters. In Ref. [12] a maximum available pulse repetition rate of the LISOL laser system of 200 Hz prevented a complete evaluation of the in-gas-jet spectroscopy benefits. Since the atom's flow velocity in the gas jet is about 200 times higher than that inside the gas cell, a higher pulse repetition rate would be required for optimum temporal overlap between the lasers and the atoms in the jet.

In this paper, we report on the results obtained in new tests of In-Gas Laser Ionization and Spectroscopy (IGLIS) studies in the supersonic gas jet expanding out of the LISOL gas cell. A series of experiments were performed at LISOL in which the ionization efficiency using a high-repetition-rate all-solid-state laser system was investigated and directly compared to that of the LISOL low-repetition-rate dye laser system in off- and on-line conditions. Such a combination of a high-repetition rate laser system with a gas cell-based ion source is currently used also at the IGISOL facility in Jyväskylä [14,15].

The new possibilities for performing high-resolution laser spectroscopic studies of exotic nuclei using the in-gas-jet based technique arouse a great interest at other present and future on-line facilities, as e.g., IGISOL (JYFL), PALIS (RIKEN), KISS (KEK), and SPIRAL2 (GANIL).

2. Experiment

Here we shall describe briefly only the front end of the LISOL setup [16] as it is of central importance for the discussion of the reported measurements. A detailed description of the entire LISOL facility can be found elsewhere [2,17,18].

A primary high-energy projectile beam from a driver cyclotron enters the gas cell through a molybdenum window and impinges on a thin target inducing nuclear reactions. The reaction products are thermalized and neutralized in the buffer gas, typically argon at a pressure of a few hundred mbar, and are transported by the gas flow towards the ionization region. A dual-chamber gas cell-type [8] was employed in these measurements (see Fig. 1). The main characteristic of this gas cell with respect to previous models is the division of the cell in two volumes; one for production, thermalization and neutralization of species, and the other for ionization. This spatial separation between the two volumes increases the in-gas-cell ionization efficiency and allows for the application of DC fields in the ionization region, thus assuring the collection of ions surviving the process of neutralization.

The atoms of the element of interest can be laser ionized in the ionization chamber and subsequently extracted through the exit hole ($\phi = 1$ mm) or, alternatively, ionization can be carried out in the expanding free jet within the rods of an RF SextuPole Ion Guide (SPIG). Owing to geometrical constraints in the present setup the laser beams can only be sent along the extraction axis and through the exit hole to interact with the atoms either inside the cell or afterwards within the SPIG (see Fig. 1). By applying a positive bias between the gas cell and the SPIG rods ions from the gas cell can be

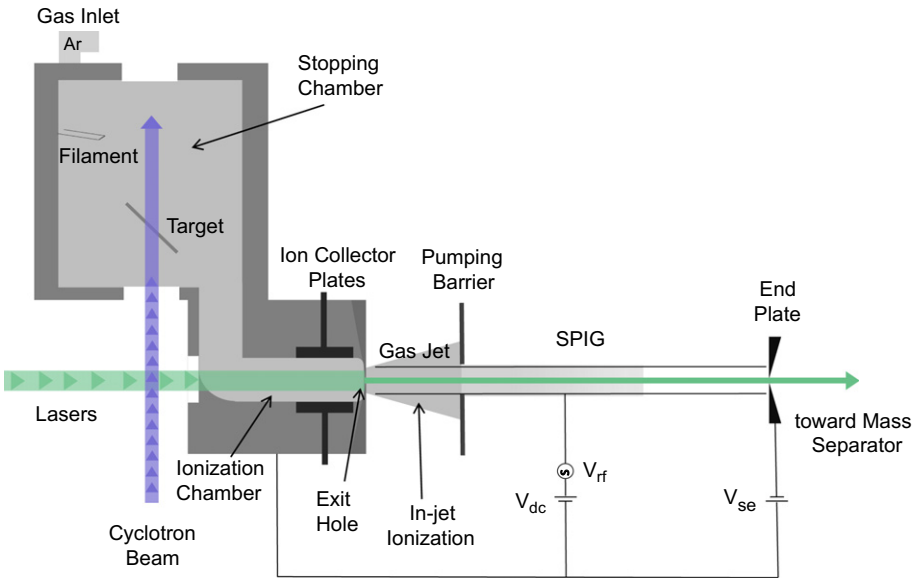

Fig. 1. Schematic layout of the laser ion source employed in these experiments. The dual chamber gas cell (separated stopping and ionization chambers) is depicted along with the primary projectile beam from the driver cyclotron and the laser beams path. Electrical connections, the expanding gas jet through the SPIG structure, and the region where in-gas-jet ionization takes place are also indicated. When V_{dc} is positive only ions produced inside the SPIG are extracted towards the mass separator. V_{se} is set for optimum extraction of the ions from the SPIG. A filament within the gas cell can be used to produce a stable atomic beam of the species of interest and perform reference measurements or off-line studies.

repelled and only those that are ionized within the RF structure (LIST mode ionization) are transported towards the mass separator. Here, the ions are selected according to their m/q value and are finally sent to the detector station. Ion collector plates within the ionization chamber can be used to collect the ions that have survived the neutralization process, thus increasing the selectivity in the process of laser ionization.

In the Leuven laser ion source program two-step two-color schemes are employed for the process of photoionization. Suitable laser radiation for atomic excitation and ionization is generated by two pulsed dye lasers (Lambda Physik Scanmate 2) pumped by two XeCl excimer lasers (Lambda Physik LPX240i) of 15 ns pulse length at a maximum repetition rate of 200 Hz [2]. Frequency doubling of the laser radiation can be achieved and is usually performed for the first step transition. Typical average pulse energies and spectral bandwidths (with additional etalon) are found to be around 3 mJ and 1.2 GHz for the fundamental radiation, and 0.3 mJ and 1.6 GHz for the second harmonic, respectively. Wavelength readout is performed by a lambdameter LM-007 from Cluster Ltd. calibrated by a single-mode He–Ne laser. A reference cell located near the optical bench can be used to produce atomic beams of stable isotopes of the species under investigation and thus to check for the matching of the resonance frequencies before the lasers are sent to the gas cell ion source, located 15 m away. A spectral range including wavelengths from 330 to 985 nm can be reached with this laser system in the fundamental wavelength and from 205 to 330 nm with second harmonic generation (SHG).

The Ti:sapphire (Ti:sa) laser system chosen for intercomparison with the LISOL lasers was commissioned in a joint collaboration between the University of Mainz and GANIL. The setup consisted of three Ti:sa lasers pumped by a frequency doubled Nd:YAG (Photonics Industries International Inc., DM75-532) of 100–200 ns pulse length and 10 kHz maximum repetition rate. The accessible wavelength range of the Ti:sa crystal covers about 680–1100 nm, however, in practice the availability of suitable mirror-sets narrowed this range to about 700–940 nm. Shorter wavelengths in the regions of 350–470 and 210–310 nm could be obtained by multi-harmonic generation. The wavelengths of the system were measured using a lambdameter (WS6/600, High Finesse). Owing to the lower gain of the Ti:sa crystal as compared to the dyes, pulse build-up times are longer and depend strongly on the laser resonator cavity conditions. Accordingly, pulses of individual lasers need to be synchronized using fast Pockels cells as resonator internal Q-switches. For the ionization step in copper, intra-cavity frequency doubling was used in one of the Ti:sa lasers increasing the SHG pulse energy to about 110 μJ. A more detailed description of this laser system can be found in Ref. [19].

The specifications of the two laser systems are summarized in Table 1. The main differences lie in the maximum pulse repetition rate and pulse energy, however, also the spectral linewidth as well as the pulse duration differ by a considerable factor in the range of two to four. All these aspects may significantly influence the ionization efficiency. Owing to the narrower overall tuning range of the Ti:sa lasers as compared to that of the dye lasers, up to third harmonic generation (THG) was necessary to accomplish suitable ionization schemes for the elements under investigation. This fact increased the gap in effective pulse energies between the two systems to nearly a factor of 100 in favor of the dye lasers.

In order to distinguish the multiple factors contributing to the laser ionization efficiency and to allow for a quantitative comparison and detailed analysis of these parameters, it was necessary to systematically adjust the parameters of both laser systems to provide comparable conditions. However, the repetition rate of the Ti:sa laser system could not be seamlessly reduced to that of the dye lasers without changing other aspects such as pulse energy and duration, or affect the spectral linewidth. A simple control of the pump laser repetition rate with questionable stability and varying pulse characteristics especially below 1 kHz or, alternatively, a pulse suppression using the Pockels cell in the Ti:sa was not feasible, as the differences in heat deposited in the Ti:sa crystal would influence the thermal lensing effect in the crystal. This in turn would affect beam pointing or focusing. Rather than suppressing pulses or reducing the repetition rate of the pump laser, a scheme of the laser pulses desynchronization was adopted to create a virtually reduced repetition rate for multistep resonance ionization. By employing three different channels of the trigger unit (BNC 565-8C) and the built- in duty-cycle function it was possible to create an alternating timing signal for the individual Pockels cells and to switch the lasers from synchronized to desynchronized mode on a-per-pulse basis. This in effect allowed control of the synchronized pulse repetition rate anywhere from 10 kHz to the sub-Hz region.

Table 1
Specifications of the two laser systems employed in these experiments. The wavelength range is given for the fundamental radiation. Energy per pulse for the second and third harmonic (SHG, THG) are also given. The value in brackets is obtained by intra-cavity doubling.

Laser specs	Ti:sa	Dye
Rep. rate (max)	10,000 Hz	200 Hz
Wavelength range	700–940 nm	330–985 nm
Pulse duration	30–60 ns	15–20 ns
Bandwidth	5 GHz	1.2 GHz
Pulse energy	300 μJ	3000 μJ
Pulse energy (SHG)	30(110) μJ	300 μJ
Pulse energy (THG)	6 μJ	–
Spot diameter	~3 mm	~ 6 mm
(With additional lens)	~ 1 mm	–

To verify the proper operation and correct tuning of the Ti:sa laser system a similar reference cell, as used for the dye laser system, was mounted on the Ti:sa laser table. This reference cell used a simple indirectly heated graphite oven to provide an atomic beam of the element of choice, i.e. cobalt or copper, with a crossed beam ionization geometry and a secondary electron multiplier (SEM) as detector. Owing to the perpendicular geometry and the strong collimation of the atomic beam, this reference cell could also be used as a wavelength reference to estimate line-shifts in the spectroscopy studies performed in the gas cell and in the gas jet.

The Ti:sa laser system was placed on a laser table located in the LISOL hall at a distance of 18 m from the laser ion source. A set of five right-angle uncoated prisms were used to transport the (Ti:sa and dye) laser beams up to the gas cell. Multiple partial reflections at the surfaces of the prisms resulted in a measured 60% total transmission. The second of these prisms was placed on a beam splitter mount that served to choose which of the well overlapped beams from the different laser systems were sent to the source. An optional focusing lens ($f = 1$ m) was used in some cases (where noted) to reduce the spot diameter and improve the ionization efficiency of the Ti:sa laser beams. This stronger focusing of the beam spot increased the difference of excitation volumes up to a factor of 36 between the two laser systems (see Table 1).

In these experiments, high-purity argon (<1 ppb) was used as a buffer gas at a pressure of 150 mbar. Under this pressure and with a 1 mm exit hole the evacuation time of the cell is found to be around 80 ms. Filaments of cobalt and copper were installed in the gas cell for production of atoms by resistive heating of the stable isotopes ^{59}Co and ^{63,65}Cu, respectively, to be used in the off-line experiments. Once selectively ionized, these ions were mass analyzed and counted using a SEM detector. For the on-line run the cobalt filament had to be removed to allow for the necessary room to install the target holder. The CYCLONE110 cyclotron delivered a primary beam of ^{3}He^{+} (25 MeV, 1μA) to the LISOL facility that

was used in combination with a Ni target (5 μm thick, 68% natural abundance of ^{58}Ni) to produce the isotope ^{59}Cu ($T_{1/2}$ = 82 s). During the on-line studies the laser ions were mass separated and transported up to a tape station [20] for detection via their characteristic decay radiation.

3. Results

Following the optimization of both laser systems, saturation measurements were performed off-line along with a direct comparison of ionization efficiencies for the two laser setups at different pulse repetition rates. In addition, spectroscopy studies using the high repetition laser system were also carried out. Subsequent absolute ionization efficiencies, isotope production, and selectivities, were compared in on-line conditions. Furthermore, relative efficiency ratios between in-gas-cell and in-gas-jet ionization for the high repetition laser system were also determined.

3.1. Off-line experiments

The ionization schemes employed in these measurements are shown in Fig. 2. In addition to the wavelengths and level assignments, the transition rate coefficient A are also indicated were known [2,21]. For all schemes the ionization process was carried out via autoionizing states.

3.1.1. Ionization of cobalt

A different scheme, three-step three-color, had to be used for the ionization of ^{59}Co with the Ti:sa lasers due to an unsuitable wavelength of the second step transition in the scheme adopted by the dye lasers. Measurements of the in-gas-cell ionization dependency on the average laser-pulse energy were taken for this ionization scheme with all three laser frequencies fixed on resonance. The results are shown in Fig. 3. The solid lines represent the best fit to the data points of the function [22]

$$N = N_0(1 - \exp(-E/E_{sat})),$$

from which one can estimate the average energy per pulse E_{sat} required to saturate the corresponding atomic transitions. Notice that the saturation values given in Fig. 3 ($E_{sat}^{1/2} = E_{sat} \cdot ln2$) represent the average energy per pulse to obtain an excitation or ionization efficiency of 50%.

While first and second steps were fully saturated, no indication of saturation was observed for the third step. In the case of the dye laser system both corresponding steps were fully saturated with the available laser power.

The production of ^{59}Co$^+$ as a function of the pulse repetition rate of the two different laser systems are shown in Fig. 4 (top). The results display a linear increase of the ionization signal for the Ti:sa lasers, while for the dye lasers the signal reaches a saturation point at about 100 Hz, indicated by the intersection of two straight lines. This saturation value for the dye lasers can be ascribed to an evacuation time of the irradiated volume in the ionization chamber of about 10 ms [8] in combination with a sufficient energy of the dye laser to saturate both atomic transitions. Accordingly, 100 Hz is sufficient to irradiate all atoms and ionize the full volume covered by the lasers. For the Ti:sa lasers, however, at 100 Hz repetition rate the ionization efficiency is 200 times smaller than that for the dye lasers. Hence, 10 kHz (a 100 times higher frequency) are not enough to ionize all the atoms in the ionization volume covered by the laser beams. This observed lower ionization efficiency of the Ti:sa laser system at 10 kHz compared with that of the dye lasers at 200 Hz, can therefore be attributed to the non-saturation of the third step transition in the adopted ionization scheme (cf. Fig. 3).

3.1.2. Ionization of copper

For these measurements both laser systems could use the same ionization scheme (see Fig. 2) making a direct comparison between their performances possible. Saturation of both atomic transitions was obtained by the dye lasers, while for the Ti:sa lasers the available average energy per pulse of about 6 μJ of the frequency tripled light for the first step transition was insufficient to reach saturation. Fig. 5 illustrates the results obtained for the ion signal as a function of the available pulse energy for the two laser systems. Differences in saturation energy for the second step in the two laser systems can be explained by a significant deviation of the laser spot size, which was measured to be around a factor of two to three larger in diameter for the dye lasers.

As previously, ion production was measured as a function of the repetition rate for both laser systems. The results are shown in Fig. 4 (bottom). Again, the available power of the dye lasers (440 μJ and 3.9 mJ for the first and second transition, respectively) provided saturation behavior since a single irradiation of the ionization chamber was sufficient to ionize the full volume covered by the laser beams with a 120 Hz repetition rate. The increase to 120 Hz in the required pulse repetition rate compared to the 100 Hz observed in the ionization of cobalt (Fig. 4 (Top)) can be attributed to the weaker saturation of the first step transition in the atomic scheme of copper with respect to that of cobalt. For the Ti:sa lasers operated at 120 Hz the ionization signal is once again around 200 times smaller than for the dye lasers at the same repetition rate, consequently the ionization of all atoms in the laser

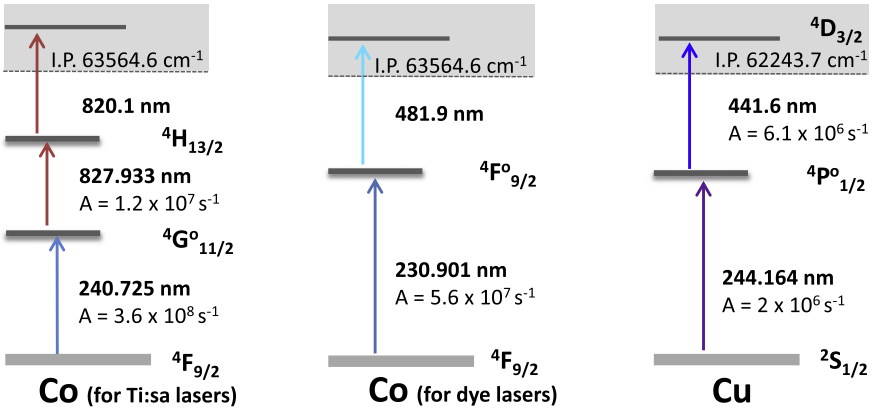

Fig. 2. Adopted ionization schemes. For the ionization of copper the same scheme was used by the two laser systems. Wavelengths (in air), level assignments, and the transition rate coefficient A are given [2,21]. See text for details.

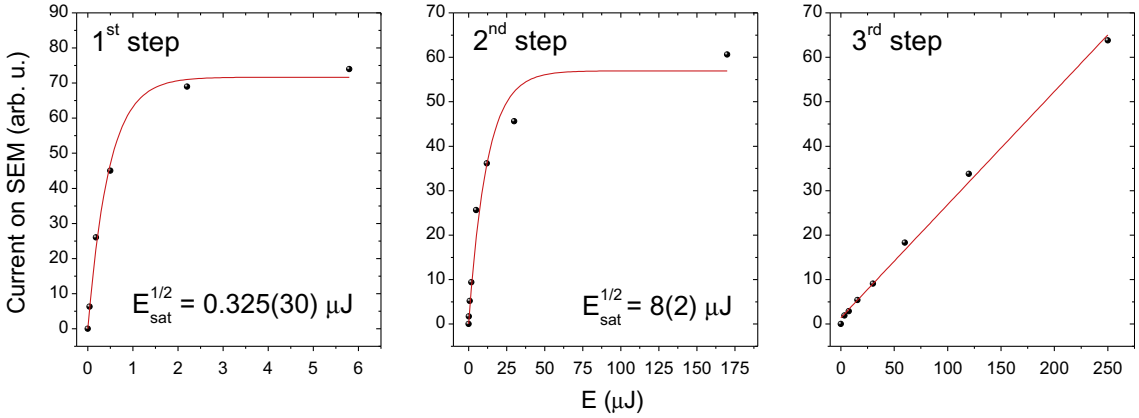

Fig. 3. Ion signal as a function of the average energy per pulse for the three transitions used in the ionization scheme of cobalt with the Ti:sa lasers (@ 10 kHz). Fits to the data points (solid line) were used to obtain $E_{sat}^{1/2}$ of the atomic transitions, corresponding to the energy per pulse needed to obtain an excitation or ionization efficiency of 50%.

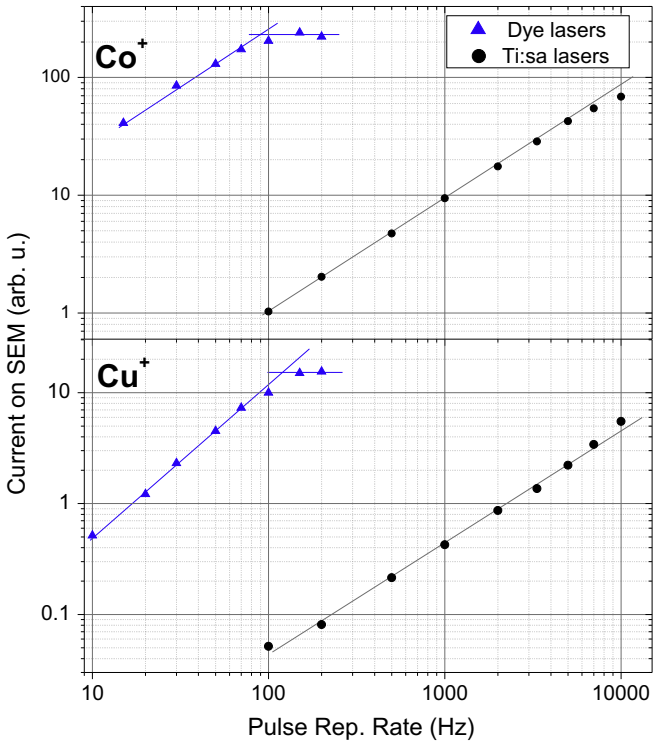

Fig. 4. Results obtained in off-line experiments for the dependence of the ion signal with the pulse repetition rate of both laser systems in the ionization of cobalt (top) and copper (bottom).

ionization volume at the maximum repetition rate of 10 kHz was also impossible here. This results in the linear trend observed in Fig. 4 (bottom), predominantly caused by the lack of available laser power to saturate the first step transition.

To better understand the linear behavior shown by the Ti:sa lasers one can try to reproduce the experimental results by using a simple model, accounting only for the duty cycle efficiency, to represent the total laser ionization efficiency ϵ_{tot} as a function of the pulse repetition rate p_{rr}. If laser ionization is performed with a given efficiency per pulse ϵ_p, after a first irradiation of the ionization volume the fraction of neutrals present will be 1-ϵ_p. If owing to the higher repetition rate this volume is irradiated a number of times $k = p_{rr} \cdot \tau_e$, given by the product between the pulse repetition rate and the evacuation time (τ_e =10 ms) of the ionization chamber, one can estimate the total efficiency for a given repetition rate beyond $1/\tau_e$ as follows (for smaller values of p_{rr} a linear dependence is assumed):

$$\epsilon_{tot} = 1 - (1 - \epsilon_p)^k, \quad (1)$$

Fig. 6 displays the results after applying Eq. (1) for a number of laser settings differing in pulse ionization efficiency ϵ_p. By comparing these results with those from Fig. 4 one could explain the observed linear trend in the Ti:sa lasers to be caused by a low efficiency per pulse, which according to the measured factor of 200 between total ionization efficiencies for the two laser systems, could be considered to be about 0.5%. In this calculation we have assumed a total efficiency of 100% for the dye lasers at a repetition rate of 100 Hz. This assumption is only true for the volume covered by the laser beams, approximately 6 mm in diameter, which only represents around 40% of the total volume of the ionization chamber.

3.1.3. An attempt to laser spectroscopy with the Ti:sa laser system

Frequency scans of the first step transition in copper were taken with the Ti:sa lasers in three different locations (reference cell, gas cell, and SPIG) in order to directly observe the benefits on the spectral resolution of in-gas-jet laser spectroscopy. With a fundamental linewidth of more than 5 GHz, the Ti:sa laser system did not poses the wavelength resolution required to resolve the hyperfine structure (HFS) of copper. In a first scan of the HFS of ^{63}Cu only a single peak was visible, indicating a linewidth of more than 15 GHz for the frequency-tripled light that masked the hyperfine structure completely. To reduce the laser bandwidth a dichroic mirror of unknown reflectivity was installed into the cavity of the Ti:sa laser as an additional etalon for wavelength selection. With the new configuration, scans were taken in the reference cell, gas cell, and SPIG (in the gas jet). Though the accuracy with this method certainly was not enough to determine the A and B coupling constants of the hyperfine structure with satisfying precision, relevant information about line widths and shifts due to the Doppler effect and to the argon pressure was gained.

Frequency scans of the first step transition for the Ti:sa system in the three different locations are shown in Fig. 7 with a summary of the results obtained. For the frequency scans, and later on for the on-line comparison between the two lasers, an additional focusing lens was installed at the entrance of the gas cell vacuum chamber, thus reducing the beam spot of the Ti:sa lasers to about 1 mm in diameter. As a sample of natural copper was employed in the reference cell, a sum of two hyperfine structures weighted with the natural abundance of $^{63-65}$Cu and separated by an isotope shift of 0.977(21) GHz [10] was used in the fits. For the results in the gas

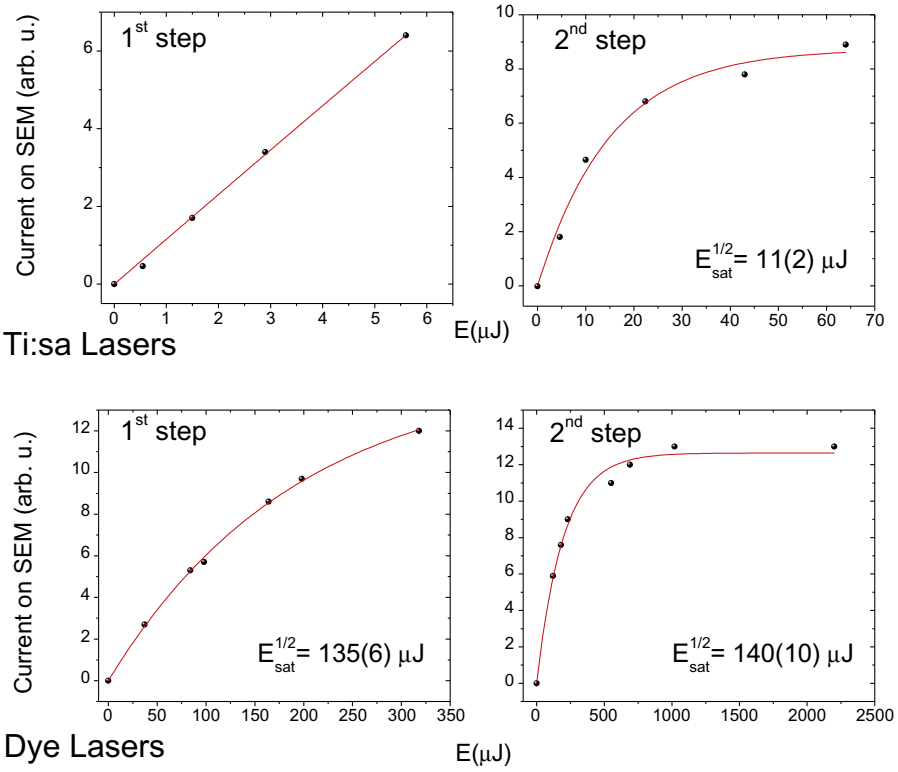

Fig. 5. Ion signal as a function of the average energy per pulse for the two transitions employed in the ionization scheme of copper. Corresponding saturation energies were extracted from fits of the theoretical behavior to the data points. The top panel shows the results for the Ti:sa lasers (@ 10 kHz) with a first step transition that is not saturated. The saturation curves for the dye lasers (@ 50 Hz) are shown in the bottom panel.

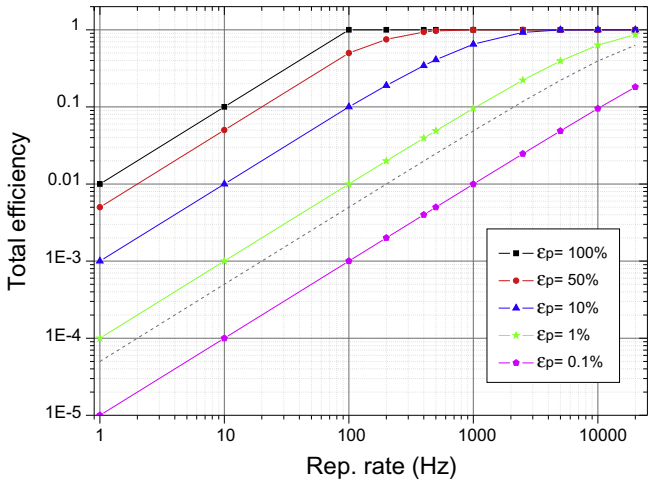

Fig. 6. Results obtained from simulations of the total ionization efficiency as a function of the pulse repetition rate for various laser settings differing in pulse ionization efficiency ϵ_p. The dashed line illustrates the expected total efficiency of the Ti:sa laser with an efficiency per pulse of 0.5% estimated according to the measured ratio of efficiencies of both laser systems.

cell and the SPIG, a pure ^{63}Cu HFS was assumed as the ion beam was filtered in the mass separator. The vertical line indicates the center of gravity (CoG) for the reference cell scan with a value of 1227 458.9(1) GHz, which was found to be in reasonable agreement with the literature value of 1227 462(3) GHz [23]. Owing to the high laser bandwidth, the limited statistics, and considering that errors do not include any systematic calibration errors of the wavemeter (High Finesse WS/6) no quantitative analysis of this value was attempted.

The resonance linewidth in the gas jet is practically dominated by the laser bandwidth, as can be seen by comparison with the resonance in the reference cell, however, additional residual Doppler and power broadening could also be present in both spectra.

For the resonance in the gas cell a clear effect of pressure broadening along with a pressure shift with respect to the reference cell are observed. The shift seems to be in the opposite direction to that previously measured in [12] with the dye laser system. The errors are relatively large, compared to the small shift, but there is a plausible reason behind this irregular shift. As the Ti:sa system is strongly focused, the ionization is likely to occur in the center of the laminar gas flow stream close to the exit hole, where the flow velocity could already be high enough for the Doppler effect to counteract the pressure shift. In fact, by measuring the relative shift of the gas cell signal with respect to that in the reference cell one can estimate a value for the velocity of the atoms in the irradiation volume to be v_{gc} = 220(80) m/s. To determine a total relative shift of 0.9(3) GHz we have used the expected pressure shift of Cu atoms irradiated in the gas cell filled with argon at a pressure of 150 mbar, which amounts to −0.30(15) GHz [12]. A better study of these effects would require a much narrower laser, found e.g. in an injection locked Ti:sa laser [24] or by amplification of a continuous wave laser, operated with a precise frequency control using a Fabry–Perot-Interferometer or similar devices [25].

According to the frequency shift observed in the gas-jet resonance of 2.5(3) GHz the velocity of the atoms in the gas jet can be determined to be v_{jet} = 600(50) m/s, in agreement with previous results using the dye lasers [12].

3.2. On-line experiments

A comparison of the performance for in gas cell ionization between the two laser systems was also carried out under on-line

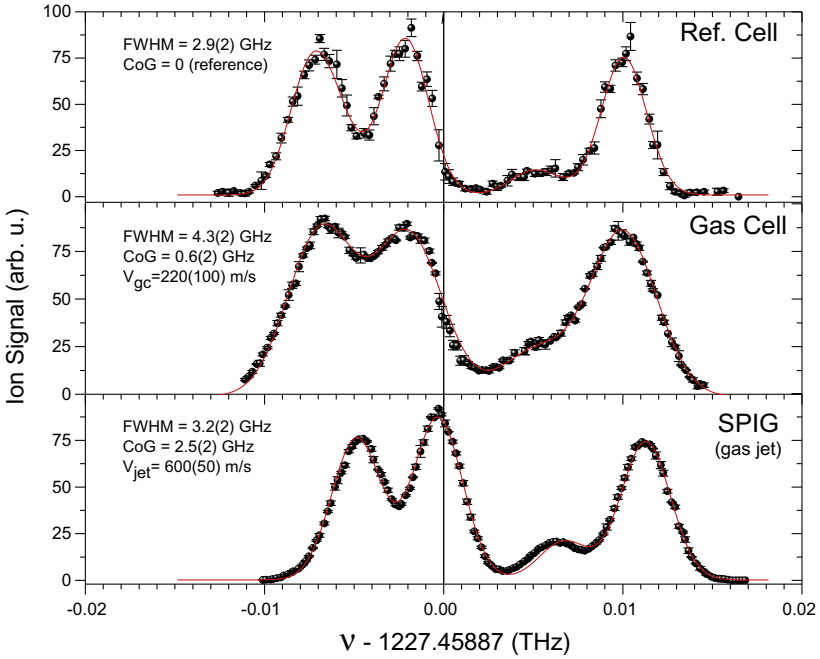

Fig. 7. Frequency scans using the Ti:sa lasers of the first step transition in copper obtained in three different locations; reference cell, gas cell, and SPIG (in the gas jet). The fits to the data points are also shown. A combination of two etalons was used to reduce the laser bandwidth to a value of less than 3 GHz (THG) and thus the hyperfine splitting could be resolved. A vertical line indicating the center of gravity (CoG) of the reference cell data is shown to guide the eye through the relative shift in the position of the peaks for each scan at a different location. Similar spectra for nickel taken with the dye laser system can be found in [12].

conditions using the short-lived ^{59}Cu isotope. The isotope of interest was produced in the nuclear reaction ^{58}Ni(^{3}He-25 MeV, np)^{59}Cu, with a calculated cross section of 120 mb [26]. The expected isotope yield was calculated after considering the energy loss of the primary beam in the different intersecting surfaces and gas volume up to the back of the target. The remaining energy resulted in an effective target thickness of 0.32 mg/cm^2 and in an expected yield of 1.7×10^6 atoms/pμC of ^{59}Cu that recoiled from the target to the gas cell volume.

As mentioned above a focusing lens (f = 1 m) was employed for the on-line comparison between the two lasers. With this lens the beam spot was reduced and the saturation of the first step transition was significantly improved for the Ti:sa lasers to the detriment of a better spatial overlap.

A problem with the excimer pump lasers during the on-line experiments reduced the performance of the dye lasers and hampered the direct comparison between the two laser systems. As a consequence of this problem a laser power reduction by a factor of four (down to 100 μJ per pulse) and three (1.3 mJ per pulse) was measured for the first and second step transitions, respectively, compared to the working conditions during the off-line experiments. As illustrated in Fig. 5, a pulse energy reduction down to 1.3 mJ for the second step laser does not alter the ionization efficiency. For the first step, however, the power reduction is significant and its effect on the ionization efficiency can be estimated from the saturation curve to be about 40% of the ionization efficiency in saturation conditions, as measured during the off-line experiments. In order to properly quantify the performance of the dye lasers a proportionality factor of 2.3 was applied accordingly to the data obtained in the on-line run.

The on-line studies started with a comparison of the recorded number of β counts as a function of the primary beam current. The results of these measurements are shown in Fig. 8(a). One can observe a significant improvement in the ionization efficiency with the Ti:sa lasers due to the implementation of the additional focusing lens. Contrary to the results obtained in the off-line tests (see Fig. 4) the relative ionization efficiency of both laser systems was found to be comparable. On top of that, the linear trend observed in the figure indicates no influence of high plasma density or gas impurities on the ion production, as expected from using a dual-chamber-type gas cell.

Fig. 8(b) shows the results obtained on the dependence of the β activity on the pulse repetition rate. From these results one can infer that the Ti:sa lasers complement the low available power and small beam spot with their higher repetition rate. Accordingly, the ion production by the two laser systems is comparable. Notice here that saturation of the ionization signal for the dye lasers is not observed owing to the reduced laser power caused by the problem with the excimer lasers. On the other hand, the lack of saturation for the improved ionization signal of the Ti:sa laser with respect to that in off-line conditions can be understood owing to the strong focusing of the lasers on a volume of high atom density in the proximity of the exit hole, as mentioned above. In this small volume with the atoms moving at a high velocity, a repetition rate of 10 kHz still is well below the value required to produce saturation.

Measurements of ion production off- and on-resonance were carried out with both laser systems for different (on/off) ion collector settings. The pulse repetition rate of the Ti:sa lasers was fixed at 10 kHz and that of the dye lasers at 150 Hz. With the obtained values for the production of ions, ion selectivities were calculated and, along with the expected yields, absolute production efficiencies determined. The results of these measurements are summarized in Table 2. As expected from the aforementioned on-line results the ion production with both laser systems was found to be very similar, with the same on-resonance production efficiency of 0.6%. A background count rate of about 0.5 Hz was registered in the β-detector during the measurements, which was subtracted to obtain the production rates reported here. Values for selectivities of about 450(50), for ion collector off, were also found to be comparable between both laser systems.

A key point during the on-line run was to check the capabilities of the high repetition lasers for in-gas-jet ion production and

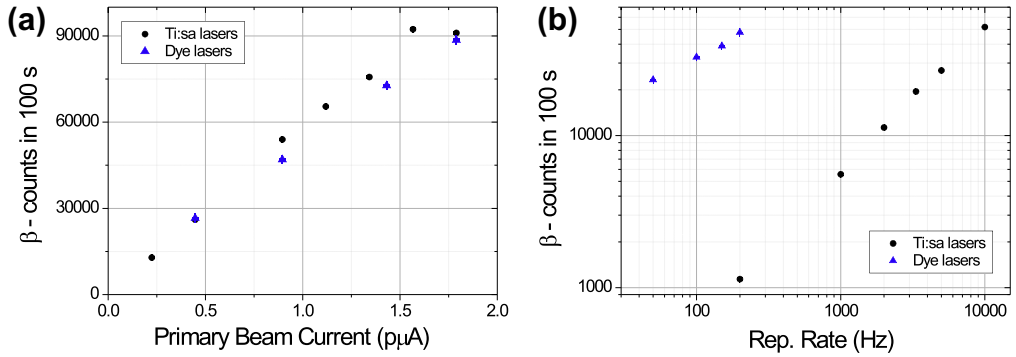

Fig. 8. (a) Activity of ^{59}Cu registered as a function of the cyclotron beam current for the Ti:sa lasers at 10 kHz and for the dye lasers at 150 Hz. The count rate using the dye has been corrected for the laser-power reduction (see text). (b) On-line comparison of the dependence of the β activity on the pulse repetition rate.

Table 2
Summary of the on-line results obtained when comparing the two laser systems (first column) in the ionization of ^{59}Cu in the gas cell. Second and third columns specified the lasers and ion collector settings, respectively. Deduced productions along with the statistical errors are given in the third column and total production efficiencies in the last column.

Laser system	Lasers	Ion col.	P (at/s)	ϵ (%)
Ti:sa Lasers	Off	Off	26(2)	1.5×10^{-3}
	On (@10 kHz)	Off	10,630(40)	0.6
	Off	On	1(1)	1×10^{-4}
Dye Lasers	Off	Off	21(2)	1.2×10^{-3}
	On (@150 Hz)	Off	10,000(40)	0.6
	Off	On	1(1)	1×10^{-4}

compare it to that within the gas cell. The selection of in-gas-jet ionization signal was performed by applying a positive bias voltage V_{dc} between the gas cell and the SPIG rods (see Fig. 1). Prior to the measurements of in-gas-jet ion production a series of measurements were performed to determine the proper blocking bias voltage, which was found to be around 40 V (see Fig. 9(a)). Notice that for in-gas-cell ionization (Fig. 8) V_{dc} is set to −180 V for an optimum extraction of the ions from the gas cell. Applying the blocking bias we studied the ionization signal as a function of the pulse repetition rate. With the Ti:sa lasers operated at maximum repetition rate a fairly high ionization signal was obtained (see Fig. 9(b)), resulting in an ion production of 165(6) at/s. This value, 60(3) times smaller than that obtained by in-gas-cell ionization, results in an absolute in-gas-jet ionization efficiency of 0.01%.

Unfortunately we could not perform a direct comparison of the ionization in the gas jet between the two laser systems owing to the mentioned loss in laser-power of the dye lasers, which at this point in time were inactive as no reliable performance could be assured. In any case, the spatial overlap in the gas cell is a factor of about 36 larger for the dye laser due to the difference in laser spot diameters, which leaves a smaller amount of available neutrals for the ionization in the gas jet. On the other hand, the temporal overlap between lasers and atoms in the gas jet is a factor of 50 smaller owing to the difference in pulse repetition rate. These two facts make the expected reduction factor to be significantly larger for the dye lasers.

In previous results obtained with the dye lasers [12] a reduction factor of 450(20) was found between the ionization in the gas cell and in the gas jet. A comparison between the performance of the two laser systems using this result is meaningless as the data was taken in a completely different gas cell geometry to that of the dual chamber.

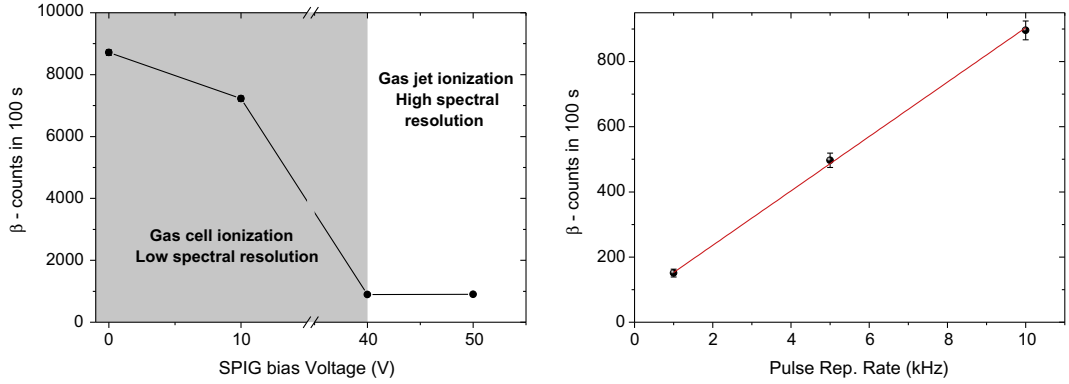

Fig. 9. (a) Ions signal measured with the Ti:sa lasers as a function of the bias voltage applied between the gas cell and the SPIG rods. A voltage of 40 V is sufficient to block the ions from the gas cell and select only those ionized in the gas jet with optimal conditions for laser spectroscopy studies. (b) In-gas-jet ionization signal using the Ti:sa lasers at different pulse repetition rates.

4. Summary and conclusions

Stable Co and Cu isotopes were ionized in the gas cell by two different laser systems in off-line experiments showing favorable results for the dye laser system given the sufficient available laser power to saturate all atomic transitions. A stronger focusing of the Ti:sa laser beams could be used to increase the low ionization efficiency per pulse observed in off-line conditions resulting in a comparable performance of both laser systems in the on-line measurements.

Primary limitations experienced in previous tests that concealed the overall capabilities of in-gas-jet laser ionization and spectroscopy studies could be partially mitigated after the experiments reported here owing to the significant improvement of the time-overlap efficiency using the Ti:sa lasers, which provided a reasonable ionization efficiency in the gas jet. Unfortunately, these data could not be directly contrasted with the performance of the dye lasers in these experiments or with previous ones, in which a different gas cell geometry was employed. Furthermore, the fact that the ionization in the gas cell using the Ti:sa lasers was performed on an unknown volume very close to the exit hole made an estimation of a reduction factor considering the spatial and temporal overlap efficiencies impossible.

The departure from unity of the measured reduction factor (60(3)) cannot only be attributed to geometrical restrictions as the Ti:sa lasers were strongly focused and the laser beams were not limited by the gas cell exit hole, which could result in a similar interaction volumes in the gas cell and in the gas jet. The reduction of ionization rate observed in the gas jet points towards the importance of using a different exit hole geometry to assure a better spatial overlap. Calculations of the atom density distribution of a free jet expanding out of the gas cell [27] indicate that the effective ionization length within the RF structure is less than 10 mm. Instead of requiring a laser system with a pulse repetition rate well above 10 kHz to fully optimize the ionization efficiency in the gas jet, a more feasible solution would be to use a *de Laval* nozzle, or another type of nozzle geometry in the gas cell exit hole. The former kind of nozzles have proven to be able to produce collimated gas jets of a few centimeters in length [28].

In addition, frequency scans were performed in the gas jet using the high repetition rate Ti:sa laser system. These measurements showed a well resolved hyperfine splitting of the ground and excited states of ^{63}Cu, only limited in resolution by the intrinsic laser bandwidth and possible residual Doppler broadening. Along with the corresponding optimization of temporal and spatial overlaps these results show the promise of in-gas-jet laser ionization becoming a powerful tool for future spectroscopic studies at on-line facilities making use of gas-cell-based laser ion sources. Open questions regarding the limitations of this method for laser spectroscopy experiments will be addressed by future studies employing higher resolution laser systems such as the injection-locked Ti:sa lasers developed at the University of Mainz [24] or the amplification of continuous wave single mode radiation in a pulsed dye amplifier currently under investigation at LISOL [25].

Acknowledgments

We thank the CRC team, Louvain-La-Neuve (Belgium), for providing the primary beams. This work was supported by FWO-Vlaanderen (Belgium), by GOA/2010/010 (BOF KULeuven), by the IAP Belgian Science Policy (BriX network P6/23), by the European Commission within the Seventh Framework Programme through I3-ENSAR (contract No. RII3-CT-2010–262010), by the French Research National Agency (ANR) under contract No. ANR-08-BLAN-0116-01, and by a Grant from the European Research Council (ERC-2011-AdG-291561-HELIOS).

References

[1] M. Huyse, R. Raabe, J. Phys. G. 38 (2011) 024001.
[2] Yu. Kudryavtsev, J. Andrzejewski, N. Bijnens, S. Franchoo, J. Gentens, M. Huyse, A. Piechaczek, J. Szerypo, I. Reusen, P. Van Duppen, P. Van Den Bergh, L. Vermeeren, J. Wauters, A. Wöhr, Nucl. Instr. Meth. B 114 (1996) 350.
[3] M. Facina, B. Bruyneel, S. Dean, J. Gentens, M. Huyse, Yu. Kudryavtsev, P. Van den Bergh, P. Van Duppen, Nucl. Instr. Meth. B 226 (2004) 401.
[4] I. Reusen, A. Andreyev, J. Andrzejewski, N. Bijnens, S. Franchoo, M. Huyse, Yu. Kudryavtsev, K. Kruglov, W.F. Mueller, A. Piechaczek, R. Raabe, K. Rykaczewski, J. Szerypo, P. Van Duppen, L. Vermeeren, J. Wauters, A. Wöhr, Phys. Rev. C 59 (1999) 2416.
[5] S. Dean, M. Górska, F. Aksouh, H. de Witte, M. Facina, M. Huyse, O. Ivanov, K. Krouglov, Yu. Kudryavtsev, I. Mukha, D. Smirnov, J.-C. Thomas, K. Van de Vel, J. Van de Walle, P. Van Duppen, J. Van Roosbroeck, Eur. Phys. J. 21 (2004) 243.
[6] S. Franchoo, M. Huyse, K.-L. Kratz, K. Kruglov, Y. Kudryavtsev, W.F. Mueller, B. Pfeiffer, R. Raabe, I. Reusen, P. Van Duppen, J. Van Roosbroeck, L. Vermeeren, W.B. Walters, A. Wöhr, Phys. Rev. Lett. 81 (1998) 3100.
[7] Yu. Kudryavtsev, T.E. Cocolios, J. Gentens, O. Ivanov, M. Huyse, D. Pauwels, M. Sawicka, T. Sonoda, P. Van den Bergh, P. Van Duppen, Nucl. Inst. Meth. B 266 (2008) 4368.
[8] Yu. Kudryavtsev, T.E. Cocolios, J. Gentens, M. Huyse, O. Ivanov, D. Pauwels, T. Sonoda, P. Van den Bergh, P. Van Duppen, Nucl. Instr. Meth. B 267 (2009) 2908.
[9] T.E. Cocolios, A.N. Andreyev, B. Bastin, N. Bree, J. Buscher, J. Elseviers, J. Gentens, M. Huyse, Yu. Kudryavtsev, D. Pauwels, T. Sonoda, P. Van den Bergh, P. Van Duppen, Phys. Rev. Lett. 103 (2009) 102501.
[10] T.E. Cocolios, A.N. Andreyev, B. Bastin, N. Bree, J. Buscher, J. Elseviers, J. Gentens, M. Huyse, Yu. Kudryavtsev, D. Pauwels, T. Sonoda, P. Van den Bergh, P. Van Duppen, Phys. Rev. C 81 (2010) 014314.
[11] R. Ferrer et al. (in preparation).
[12] T. Sonoda, T.E. Cocolios, J. Gentens, M. Huyse, O. Ivanov, Yu. Kudryavtsev, D. Pauwels, P. Van den Bergh, P. Van Duppen, Nucl. Instr. Meth. B 267 (2009) 2918.
[13] K. Blaum, C. Geppert, H.-J. Kluge, M. Mukherjee, S. Schwarz, K. Wendt, Nucl. Inst. Meth. B 204 (2003) 331.
[14] I.D. Moore, T. Kessler, T. Sonoda, Y. Kudryavstev, K. Peräjärvi, A. Popov, K.D.A. Wendt, J. Äystö, Nucl. Instr. Meth. B 268 (2010) 657.
[15] I.D. Moore, A. Nieminen, J. Billowes, P. Campbell, C.H. Geppert, A. Jokinen, T. Kessler, B. Marsh, H. Penttilä, S. Rinta-Antila, B. Tordoff, K.D.A. Wendt, J. Äystö, J. Phys. G. Nucl. Part. Phys. 31 (2005) 1499.
[16] Yu. Kudryavtsev, M. Facina, M. Huyse, J. Gentens, P. Van den Bergh, P. Van Duppen, Nucl. Inst. Meth. B 204 (2003) 336.
[17] M. Huyse, P. Decrock, P. Dendooven, J. Gentens, G. Vancraeynest, P. Van den Bergh, P. Van Duppen, Nucl. Instr. Meth. B 70 (1992) 50.
[18] L. Vermeeren, N. Bijnens, M. Huyse, Y.A. Kudryavtsev, Z.N. Qamhieh, R.E. Silverans, P. Thoen, E. Vandeweert, J. Wauters, P. Van Duppen, Phys. Rev. Lett 73 (1994) 1935.
[19] C. Mattolat, S. Rothe, F. Schwellnus, T. Gottwald, S. Raeder, K. Wendt, AIP Conf. Proc. 1104 (2009) 114.
[20] L. Weissman, J. Van Roosbroeck, K. Kruglov, A. Andreyev, B. Bruyneel, S. Franchoo, M. Huyse, Y. Kudryavtsev, W.F. Mueller, R. Raabe, I. Reusen, P. Van Duppen, L. Vermeeren, Nucl. Instr. Meth. A 423 (1998) 328.
[21] R.L. Kurucz, On-line atomic spectral line data base. Available from <http://www.pmp.uni-hannover.de/cgi-bin/ssi/test/kurucz/sekur.html>
[22] V.S. Letokhov, Laser Photoionization Spectroscopy, Academic Press, Orlando, 1987.
[23] J. Sugar, A. Musgrove, J. Phys. Chem. Ref. Data 19 (1990) 528.
[24] T. Kessler, H. Tomita, C. Mattolat, S. Raeder, K. Wendt, Laser Phys. 18 (7) (2008) 842.
[25] Yu. Kudryavtsev, R. Ferrer, M. Huyse, P. Van den Bergh, P. Van Duppen, (in preparation).
[26] A. Andreyev, Private communication.
[27] H. Ashkenas, F.S. Sherman, The structure and utilization of supersonic free jets in low density wind channels, in: J.H. Leeuw (Ed.), Fourth International Symposium on Rarefied Gas Dynamics, vol. II, Academic Press, Toronto, 1964, pp. 84–105.
[28] M. Reponen, I.D. Moore, I. Pohjalainena, T. Kessler, P. Karvonen, J. Kurpeta, B. Marsh, S. Piszczek, V. Sonnenschein, J. Äystö, Nucl. Instr. Meth. A 635 (2011) 24.